

# ION MICROBEAM FORMATION FOR STUDY OF RADIATION-INDUCED SEGREGATION AT GRAIN BOUNDARIES IN CONSTRUCTION MATERIALS

A.V. Romanenko, A.A. Ponomarov, A.G. Ponomarev

Institute of Applied Physics, National Academy of Sciences of Ukraine, Sumy, Ukraine

E-mail: romanenko@ipflab.sumy.ua

The approaches for creating focused ion beams with a high current density and near-uniform current distribution in a spot, that allows an uniform dose for further micro irradiation technique, were considered. A numerical simulation of the microbeam formation was performed taking into account the effect of nonuniform distribution of the ion beam. The calculation method for a deconvolution of the beam brightness distribution parameters was improved. Experiments to verify theoretical calculations were performed.

PACS: 29.17.-q

## INTRODUCTION

Electrostatic accelerators are widely used in studies of material behavior under strong irradiation damages [1, 2]. Ion irradiation is highly relevant to simulate a neutron irradiation [3]. The main advantage of the neutron damage simulation by means of the ion irradiation consists in a fast dose rate production (100 dpa in a few hours for megaelectronvolt heavy ions). To decrease an irradiation time it is necessary to increase a current density of ion beam. Focusing systems based on magnetic quadrupole lenses (MQL) can increase the current density by three orders of magnitude [4]. Generally, a profile of focused beam in the target plane has a Gaussian shape [5]. Therefore, the scanning procedure is necessary to get a region with a uniform dose distribution over the entire area of irradiation that leads to a decrease of effective dose of irradiation.

One of the tasks that require irradiation of microareas is an investigation of impurity segregation on grain boundaries under irradiation (Fig. 1) [6]. Possibility to irradiate a single selected grain provides a studying of segregation impurity and their moving along the grain boundary from the irradiated grain to non-irradiated one. Nuclear scanning microprobe is a unique tool for carrying out such experiments. It provides ion beams with high current density and permits to obtain a map of element distribution using the micro-PIXE technique.

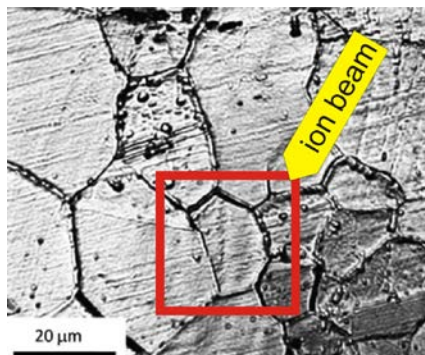


Fig. 1. Micrograph of type 304 austenitic stainless steel [6], model of ion beam microirradiation

Constant environmental conditions (vacuum) during irradiation and microanalysis, segregation formation analysis depending on irradiation dose at the early stage are ones of advantages of the nuclear microprobe application for these tasks. Introduction of the uniform dose

is one of the main requirements for the irradiation. Therefore, creating the focused ion beams with uniform distribution in a spot is an actual problem that consists of two tasks. The first one is to define a charged particles distribution in the phase volume occupied by the beam at the entrance to a probe forming system (PFS). The second task is to find the conditions for beam formation on the target with uniform current density distribution. The present work is devoted to a solution of these tasks.

## 1. DECONVOLUTION OF THE BEAM BRIGHTNESS DISTRIBUTION PARAMETERS AT THE ENTRANCE TO PROBE-FORMING SYSTEM

A method of the deconvolution of the beam brightness distribution parameters at the entrance to PFS based on the beam current distribution measurements was described in details in [4]. It was used to study an effect of a beam particles distribution on the microprobe resolution. Proposed method is applied for obtaining the brightness distribution in a small paraxial region. It assumes an overlapping of independently movable slit jaws of collimators relative to the geometrical axis, when a displacement of jaws can take on a negative value (the minimum values of  $-60 \mu\text{m}$  were used in work [4] to study a central part of the beam with the  $200 \times 200 \mu\text{m}$  size). However, a conventional design of the collimators doesn't ensure the required overlapping for measuring the overall beam region. Therefore, the earlier developed method was modified in this work.

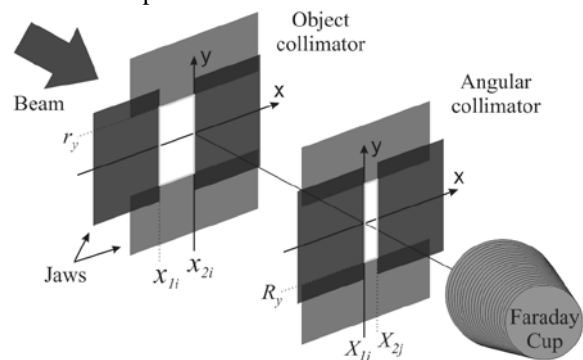


Fig. 2. Scheme of current beam distribution measurement in the plane  $xOy$  at the microprobe channel

Measurements were carried out at the IAP's "SOKOL" electrostatic accelerator of the Van de Graaff type for a 1 MeV proton beam [7]. Fig. 2 shows a sche-

matic arrangement of the object and angular collimators for the beam current distribution measurements. Both collimators are designed as two mutually perpendicular slits. At first, the collimators were positioned with some error with respect to the beam axis by measuring the maximum current for the collimator window dimensions of  $100 \times 100 \mu\text{m}$ . The direct current measurements were performed using a current integrator.

The charged particles in most plasma ion sources have Maxwellian velocity distribution. In this case the particle phase density follows normal distribution.

Since ion sources and electrostatic accelerators are axially symmetric, and the beam transportation optics has a very low level of aberrations, the brightness distribution in the four-dimensional phase space  $(x, y, x', y')$  can be represented as a product of two distributions in  $(x, x')$  and  $(y, y')$  planes

$$b(x, y, x', y') = b_0 \cdot b_x(x, x') \cdot b_y(y, y'), \quad (1)$$

where

$$b_\tau(\tau, \tau') = \exp \left[ -\frac{1}{2(1-\kappa_\tau^2)} \left( \frac{(\tau - \tau_0)^2}{\sigma_\tau^2} - 2\kappa_\tau \frac{(\tau - \tau_0)(\tau' - \tau'_0)}{\sigma_\tau \sigma_{\tau'}} + \frac{(\tau' - \tau'_0)^2}{\sigma_{\tau'}^2} \right) \right];$$

$\tau = (x, y)$ ;  $b_0$  is the axial brightness;  $\tau_0, \tau'_0$  are the collimator positioning errors;  $\sigma_\tau, \sigma_{\tau'}$  are the standard deviations;  $\kappa_\tau$  is a correlation coefficient between  $\tau$  and  $\tau'$ ;  $b_0, \tau_0, \tau'_0, \sigma_\tau, \sigma_{\tau'}, \kappa_\tau$  ( $\tau = (x, y)$ ) are the beam brightness distribution parameters deconvolved from beam current measurements.

The beam current that passed through the object and the angular collimators with the window dimensions presented in Fig. 2 is

$$\Omega_{x,ij}(\mathbf{a}_x) = \alpha_x \cdot \int_{x_{1i}}^{x_{2i}} \int_{(X_{1j}-\mu)/A}^{(X_{2j}-\mu)/A} b_x(\mu, \nu) \cdot d\nu \cdot d\mu, \quad (2)$$

where  $\mathbf{a}_x = \{\alpha_x, \sigma_x, x_0, \sigma_{x'}, x'_0, \kappa_x\}$  is a vector of deconvolved parameters of the beam brightness distribution in the phase plane  $(x, x')$ ;  $x_{1i}, x_{2i}$  are coordinates of the left and right jaws of the vertical slit of the object collimator respectively;  $X_{1j}, X_{2j}$  are coordinates of the left and right jaws of the vertical slit of the angular collimator respectively,

$$\alpha_x = b_0 \cdot \int_{-r_y}^{r_y} \int_{(-R_y-\mu)/A}^{(R_y-\mu)/A} b_y(\mu, \nu) \cdot d\nu \cdot d\mu$$
 is a normalization

factor,  $r_y = 500 \mu\text{m}$ ,  $R_y = 500 \mu\text{m}$ ;  $r_y$  are constant coordinates of top and bottom jaws of the horizontal slit of the object collimator;  $R_y$  are constant coordinates of top and bottom jaws of the horizontal slit of the angular collimator;  $A$  is the distance between the object and the angular collimators;  $\mu, \nu$  are the integration parameters corresponding to the linear and angular phase coordinates respectively.

For measuring the current distribution in the  $y$  direction, one has to make the  $x \leftrightarrow y$  substitution in the expression (2). In relation (2) quantity  $\Omega_{x,ij}(\mathbf{a}_x)$  determines a beam current passed through four-dimensional phase window which is predetermined by positions of the object and angular collimator jaws. The parameters' vector

$\mathbf{a}_x$  is determined by Levenberg-Marquardt's fitting method as a result of misalignment minimization

$$\chi^2(\mathbf{a}_x) = \sum_{(i,j)=1}^{(M_x, N_x)} \left[ \frac{I_{x,ij} - \Omega_{x,ij}(\mathbf{a}_x)}{\Delta_{x,ij}} \right]^2, \quad (3)$$

where  $\mathbf{a}_x$  is the parameters' vector corresponded to the minimum of function  $\chi^2(\mathbf{a}_x)$ ;  $I_{x,ij}$  is the measured value of the beam current for a given four-dimensional phase window which is predetermined by jaws' positions  $x_{1i}, x_{2i}, X_{1j}, X_{2j}, r_y, R_y, \Delta_{x,ij}$  is an error of the beam current measurement;  $M_x, N_x$  are numbers of window variations of the object and angular collimators.

After the distribution parameters  $\sigma_x, x_0, \sigma_{x'}, x'_0, \kappa_x, \sigma_y, y_0, \sigma_{y'}, y'_0, \kappa_y$  were determined, the value of the axial brightness for each of the four-dimensional phase window was defined by the relations

$$b_{0x,ij} = I_{x,ij} / \left( \int_{x_{1i}}^{x_{2i}} \int_{(X_{1j}+\mu)/A}^{(X_{2j}-\mu)/A} b_x(\mu, \nu) \cdot d\nu \cdot d\mu \times \int_{-r_y}^{r_y} \int_{-(R_y+\mu)/A}^{(R_y-\mu)/A} b_y(\mu, \nu) \cdot d\nu \cdot d\mu \right), \quad (4)$$

$$b_{0y,ij} = I_{y,ij} / \left( \int_{y_{1i}}^{y_{2i}} \int_{(Y_{1j}+\mu)/A}^{(Y_{2j}-\mu)/A} b_y(\mu, \nu) \cdot d\nu \cdot d\mu \times \int_{-r_x}^{r_x} \int_{-(R_x+\mu)/A}^{(R_x-\mu)/A} b_x(\mu, \nu) \cdot d\nu \cdot d\mu \right).$$

The beam current in the electrostatic accelerator has temporal and spatial instability. The current instability of "SOKOL" accelerator is at the level of 16%. Therefore, the axial brightness is determined with an error in the form of

$$b_0 = \bar{b}_0 \pm \Delta b_{0rms}, \quad (5)$$

where  $\bar{b}_0$  is an average brightness value for the sum of window sizes calculated according to (4),  $\Delta b_{0rms}$  is the standard deviation.

At the beginning, the maximum value of coordinates of the slit jaws was set at the level of  $500 \mu\text{m}$ , i.e. the sizes of the both collimators were  $1 \text{ mm}$ . Then, the sizes of the object collimator  $x_{11}=500, x_{21}=0$  were set, and the current was measured at the every step of size changing of angular collimator slits. The slit step size was  $200 \mu\text{m}$ . The set was as follows:  $X_{11}=500, X_{21}=0; X_{12}=300, X_{22}=0; X_{13}=100, X_{23}=100; X_{14}=0, X_{24}=300; X_{15}=0, X_{25}=500$ . After that the slit size of the object collimator was changed by  $200 \mu\text{m}$  and the current was measured for the same set of angular collimator. The size set for the object collimator was similar one as for the angular collimator. Thus, at the end of the measurements we have obtained the current's matrix with dimension of  $M_x=5, N_x=5$ . A similar procedure was carried out for horizontal slits.

The obtained results are:

$$b_0 = (6.7 \pm 1.1) \text{ pA}/(\mu\text{m}^2 \cdot \text{mrad}^2); \sigma_x = 621 \mu\text{m}; x_0 = -49 \mu\text{m}; \sigma_{x'} = 0.088 \text{ mrad}; x'_0 = -0.016 \text{ mrad}; \kappa_x = -0.4; \sigma_y = 667 \mu\text{m}; y_0 = -11 \mu\text{m}; \sigma_{y'} = 0.098 \text{ mrad}; y'_0 = 0.001 \text{ mrad}; \kappa_y = -0.9.$$

## 2. BEAM FOCUSING SIMULATION

Formation of beams with a near-rectangular profile of current density distribution at the target is possible on condition that the ratio  $I_{FWHM}/I_0$  is not less than 90%, where  $I_{FWHM}$  is a current at a region of full width at half maximum (FWHM) in the beam profile,  $I_0$  is the total beam current at the target. Therefore, searching of object and angular collimators sizes which provide  $I_{FWHM}/I_0 > 90\%$  condition was the aim of the calculations. Simulation is based on a method of transportation  $10^7$  particles randomly distributed in the initial phase space [8]. In the present work we took into account the nonuniform distribution of particles at the PFS entrance (obtained in the previous section). The calculations were performed for 1 MeV proton beam with the maximum energy spread  $\delta_{max}=10^{-3}$ . The focusing system is four quadrupole lenses powered as a separated "Russian quadruplet" and has demagnification factor of  $23 \times 23$  and working distance of 24 cm. The total beam current over the range from 10 to 100 nA at the target was considered. As a result, the values for collimators whereby current density distribution is close to rectangular were determined (Fig. 3).

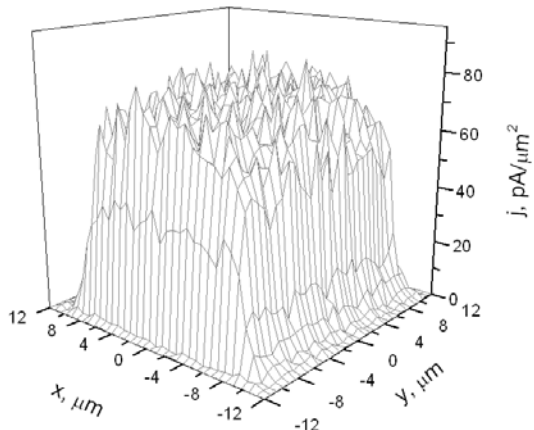


Fig. 3. Current density distribution at the target. Ratio  $I_{FWHM}$  to  $I_0$  is 95%,  $I_0 = 40$  nA

The direct on-line measurement of distribution profile is difficult to perform in practice. That is why we analyzed it by registration of secondary electron emission (SEE) during scanning of semi-infinite plates in two directions traverse to the beam (Fig. 5,a). In order to analyze experimental results we had to compare them with theoretical ones. A simple program code was used to obtain a theoretical profile of SEE and to modulate a scanning procedure of a semi-infinite plate edge with specified current density distribution [9].

## 3. EXPERIMENTAL

The measurements were performed in a nuclear scanning microprobe using a proton beam with the ion energy 1 MeV. At the beginning, exact focusing of the beam was performed by scanning the probe over a calibrated micrometric square copper mesh to obtain a stigmatic focusing. In this case, beam profile was represented by Gaussian shape. The target was replaced by two crossed blades. Scan was carried out in the square region which includes crossing point of blades. A yield of secondary electrons was registered by SEE detector. Scheme of the experiment is represented in Fig. 4.

Fig. 5,a shows the SEE map of these blades. Bright colour of edges is caused by additional SEE from edges (Fig. 6). Then we set up theoretical calculated values of collimators to obtain a uniform distribution of the current density at the target. At the final, the edges of blades were scanned and values for SEE profiles were obtained and compared to theoretical ones (Fig. 5,b,c).

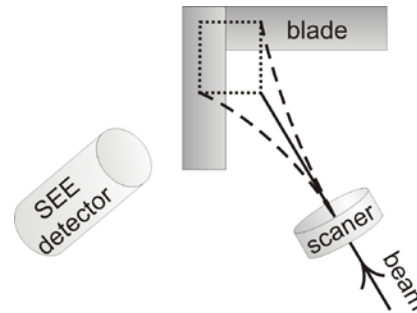


Fig. 4. Scheme of the experimental scanning of two crossed blades by 1 MeV focused proton beam. Dash line shows the region that corresponds to Fig. 5,a

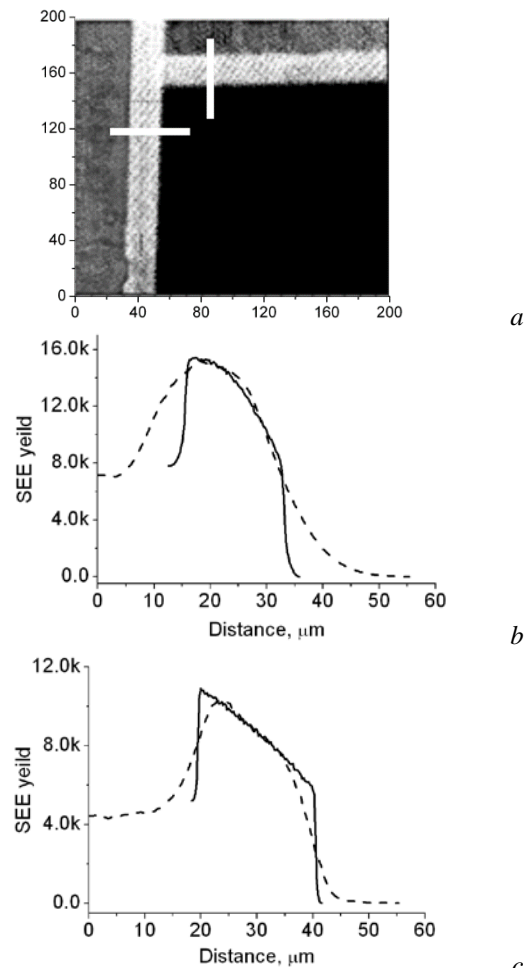


Fig. 5. Edges of the blades. a) SEE map. Lines show scanning directions. Comparison of theoretical (solid line) and experimental (dash line) SEE profiles for X (b) and Y (c) directions. Beam current was 40 nA

As can be seen, theoretical and experimental SEE profiles are in good agreement at their central part. The difference at the beginning and at the end of the shapes is caused by non-rectangular shape of the sample edges. SEE profiles strongly depend on shape of the sample (see Fig. 6).

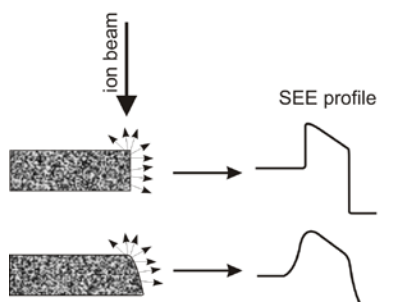


Fig. 6. Effect of a sample edge on the SEE profile for a beam with  $I_{FWHM}/I_0 = 100\%$

For the better agreement on the sides it is necessary to put into the program the exact shape of the sample (with  $\mu\text{m}$ -level precision). Stray magnetic fields may have also influenced the experimental results.

## CONCLUSIONS

The method of reconstruction of the beam brightness distribution in the object collimator plane was improved. New modified method enables to measure beam with maximum size which is only limited by the opening size of collimators. This is very important taking into account design of the collimators. This method allows deconvolution of the beam brightness distribution in full phase volume occupied by the beam.

Numerical simulations have shown feasibility of formation of ion beams with current density distribution close to rectangular. The performed experimental work confirmed the theoretical results. Some differences between theoretical and experimental results are caused by difference between edges of the real sample and its model.

## ACKNOWLEDGEMENTS

This work is performed with the support of the task program of scientific research of department of nuclear physics and energy of NAS of Ukraine "Development of perspective areas of fundamental research in nuclear, radiation physics and nuclear energy" (State registration № 0111U10610).

## REFERENCES

1. I.M. Neklyudov, B.V. Boris, V.V. Gan, G.D. Tolstolutskey. Methodology of the radiation damage simulation of the solar battery converters by electron and proton accelerators // *Problems of Atomic Sci-*

- ence and Technology. Series «Physics of Radiation Effect and Radiation Materials Science» (83). 2003, v. 3, p. 62-65.*
2. V. Permyakov, V.V. Mel'nichenko, V.V. Bryk, V.N. Voyevodin, Yu.E. Kupriyanova. Facility for modeling the interactions effects of neutrons fluxes with materials of nuclear reactors // *Problems of Atomic Science and Technology. Series «Physics of Radiation Effect and Radiation Materials Science» (90). 2014, v. 2, p. 180-186.*
3. C. Abromeit. Aspects of simulation of neutron damage by ion irradiation // *Journal of Nuclear Materials. 1994, v. 216, p. 78-96.*
4. A.A. Ponomarov, V.I. Miroshnichenko, A.G. Ponomarev. Influence of the beam current density distribution on the spatial resolution of a nuclear microprobe // *Nucl. Instr. and Meth. in Phys. Res. B. 2009, v. 267, p. 2041-2045.*
5. C.N.B. Udagama, A.A. Bettiol, J.A. van Kan, E.J. Teo, F. Watt. The rapid secondary electron imaging system of the proton beam writer at CIBA // *Nucl. Instr. and Meth. B. 2007, v. 260, p. 390-395.*
6. Parag Ahmedabadi, V. Kain, K. Arora, I. Samajdar, S.C. Sharma, P. Bhagwat. Radiation-induced segregation in desensitized type 304 austenitic stainless steel // *Journal of Nuclear Materials. 2011, v. 416, p. 335-344.*
7. V.E. Storizhko, A.G. Ponomarev, V.A. Rebrov, A.I. Chemeris, A.A. Drozdenko, A.B. Dudnik, V.I. Miroshnichenko, N.A. Sayko, P.A. Pavlenko, L.P. Peleshuk. The Sumy scanning nuclear microprobe: Design features and first tests // *Nucl. Instr. and Meth. in Phys. Res. B. 2007, v. 260, p. 49-54.*
8. A.G. Ponomarev, V.I. Miroshnichenko, V.E. Storizhko. Optimum collimator shape and maximum emittance for submicron focusing of ion beams. Determination of the probe-forming system resolution limit // *Nucl. Instr. and Meth. A. 2003, v. 506, p. 20-25.*
9. D.V. Magilin, A.G. Ponomarev, V.A. Rebrov, N.A. Sayko, K.I. Melnik, V.I. Miroshnichenko, V.Y. Storizhko. Performance of the Sumy nuclear microprobe with the integrated probe-forming system // *Nucl. Instr. and Meth. in Phys. Res. B. 2009, v. 267, p. 2046-2049.*

Article received 30.04.2015

## ФОРМИРОВАНИЕ ИОННОГО МИКРОЗОНДА ДЛЯ ИССЛЕДОВАНИЯ РАДИАЦИОННО-СТИМУЛИРОВАННОЙ СЕГРЕГАЦИИ НА ГРАНИЦАХ ЗЕРЕН В КОНСТРУКЦИОННЫХ МАТЕРИАЛАХ

А.В. Романенко, А.А. Пономарёв, А.Г. Пономарёв

Рассмотрен способ формирования сфокусированного ионного пучка с высокой плотностью тока и с распределением тока в пятне, близким к равномерному, с целью внесения равномерной дозы при микрооблучении. Проведены численные расчеты по формированию микрозонда с учетом влияния неравномерного распределения ионов в пучке. Улучшен численный метод, позволяющий восстанавливать параметры распределения яркости пучка. Проведены экспериментальные работы для верификации теоретических расчетов.

## ФОРМУВАННЯ ІОННОГО МІКРОЗОНДА ДЛЯ ДОСЛІДЖЕННЯ РАДІАЦІЙНО-СТИМУЛЬОВАНОЇ СЕГРЕГАЦІЇ НА ГРАНИЦЯХ ЗЕРЕН У КОНСТРУКЦІЙНИХ МАТЕРІАЛАХ

О.В. Романенко, А.О. Пономарьов, О.Г. Пономарьов

Розглянуто спосіб формування сфокусованого іонного пучка з великою густиною струму і з розподілом струму в плямі, що близький до рівномірного, з метою внесення рівномірної дози при мікроопроміненні. Проведено чисельні розрахунки з формування мікрозонда з урахуванням впливу нерівномірного розподілу іонів у пучку. Поліпшено чисельний метод, який дозволяє відновлювати параметри розподілу яскравості пучка. Проведено експериментальні роботи для верифікації теоретичних розрахунків.